Title

Spinal cord reconstitution with homologous neural grafts enables robust corticospinal regeneration

Journal

Nature Medicine, 22(5)

ISSN

1078-8956

Authors

Kadoya, Ken
Lu, Paul
Nguyen, Kenny
et al.

Publication Date

2016-05-01

DOI

10.1038/nm.4066

Peer reviewed

HHS Public Access

Author manuscript

Nat Med. Author manuscript; available in PMC 2016 September 28.

Published in final edited form as:

Nat Med. 2016 May ; 22(5): 479–487. doi:10.1038/nm.4066.

Spinal cord reconstitution with homologous neural grafts enables robust corticospinal regeneration

Ken Kadoya[1,2], **Paul Lu**[1,3], **Kenny Nguyen**[1], **Corinne Lee-Kubli**[1], **Hiromi Kumamaru**[1], **Lin Yao**[4], **Joshua Knackert**[4], **Gunnar Poplawski**[1], **Jennifer Dulin**[1], **Hans Strobl**[1], **Yoshio Takashima**[1], **Jeremy Biane**[1], **James Conner**[1], **Su-Chun Zhang**[4], and **Mark H. Tuszynski**[1,3,*]

[1]Department of Neurosciences, University of California - San Diego, La Jolla, CA

[2]Department of Orthopaedic Surgery, Hokkaido University, Sapporo, Japan

[3]Veterans Administration San Diego Healthcare System, San Diego, CA

[4]Waisman Center and Departments of Neuroscience and Neurology, University of Wisconsin, Madison, WI, USA

Abstract

The corticospinal tract (CST) is the most important motor system in humans, yet robust regeneration of this projection after spinal cord injury (SCI) has not been accomplished. In rodent models of SCI, we report robust corticospinal axon regeneration, functional synapse formation and improved skilled forelimb function after grafting multipotent neural progenitor cells into sites of spinal cord injury. Corticospinal regeneration requires that grafts are driven toward caudalized (spinal cord), rather than rostralized, fates. Fully mature caudalized neural grafts also support corticospinal regeneration. Moreover, corticospinal axons can emerge from neural grafts and regenerate beyond the lesion, potentially related to attenuation of the glial scar. Rodent corticospinal axons also regenerate into human donor grafts of caudal spinal cord identity. Collectively, these findings indicate that spinal cord “replacement” with homologous neural stem cells enables robust regeneration of the corticospinal projection within and beyond spinal cord lesion sites, achieving a major unmet goal of spinal cord injury research and opening new possibilities for translation.

*Correspondence to: Mark H. Tuszynski, Dept. Neurosciences, 0626, University of California - San Diego, La Jolla, CA, ; Email: mtuszynski@ucsd.edu

The authors declare that they have no competing financial interests.

Contributions

K.K. conceived and carried out experiments, interpreted the results, and wrote the manuscript. P.L. contributed to the conception of the project and performed complete transection experiments. K.N. and H.S. carried out experiments. C.L. and J.D contributed to behavior analysis. G.P. contributed to mice experiments. H.K. contributed to characterization of human NPCs. L.Y., J.K. and S.Z. contributed to generation of human NPCs from iPSCs. J.B., Y.T. and J.C. performed electrophysiological analysis. M.T contributed to the conception of the project, the interpretation of results, and wrote the manuscript.

INTRODUCTION

Despite recent progress in promoting the regeneration of many classes of central nervous system axons after spinal cord injury (SCI), the corticospinal projection remains largely refractory to regeneration[1,2]. Yet the corticospinal tract, which arises from the cerebral cortex and projects to the spinal cord, is the most important projection for voluntary movement in humans, and its failure to regenerate has been a major limiting factor in advancing potential regenerative therapies to humans. Previous reports indicate that spared corticospinal axons can sprout after injury in rodents and non-human primates [3–5], and that tissue spared by incomplete SCI can facilitate growth of some injured corticospinal axons [6,7]. However, efforts to elicit true corticospinal axon regeneration – growth of the transected axon into a spinal cord lesion cavity – have met very limited success. For example, while early life phosphatase and tensin homolog (PTEN) knockdown promotes growth of adult corticospinal axons across a small lesion gap [8], this effort fails in larger lesions that lack spared astrocyte bridges [8] and is less effective when applied after injury [9,10]. Similarly, many studies targeting Nogo receptors report modest growth or sprouting of corticospinal axons, but fall well short of promoting extensive regeneration into lesion sites themselves [6,11]. Finally, while overexpression of a neurotrophin receptor, trkB, allows corticospinal axons to regenerate into a cell graft placed in a subcortical lesion site[12], this same strategy does not accomplish regeneration into a more distantly located spinal cord lesion site [12].

The failure of corticospinal axons to regenerate stands in stark contrast to the success of experimentally induced regeneration of other descending motor systems, including the reticulospinal [13–15], raphespinal [13–16] and propriospinal [14,16] projections. Neural stem cells and neural progenitor cells (NPCs) have the potential to reconstitute lesion sites with neurons and glia [17–20]. Furthermore, they can replace lost adult neural tissue with cells homologous to the pre-injured state, either by driving them to specific regional fates [21,22] or by isolating NPCs from homologous regions of the developing nervous system[23]. We now report that homologous reconstitution of the lesioned adult spinal cord with caudalized neural stem cells or primary spinal cord-derived NPCs supports robust regeneration of corticospinal axons which form functional excitatory synapses with the neural replacement graft.

Results

Corticospinal axons extensively regenerate into neural progenitor cell grafts

We grafted GFP–labeled multipotent NPCs derived from embryonic day 14 (E14) rat spinal cord primordia (see Methods) into injury sites in six adult female Fischer 344 rats two weeks after T3 complete transection. Analysis of anterogradely-labeled corticospinal axons six weeks after grafting revealed extensive regeneration of this projection into the grafts (Fig. 1a–f). A mean of 1,650 ± 310 corticospinal axons were quantified at a distance 0.5mm within the graft (Fig. 1g, left), representing 63% of all corticospinal axons quantified 0.5mm rostral to the lesion site (Fig. 1g, right). Corticospinal axons regenerating into NPC grafts contacted dendrites of grafted cells that were labeled for MAP2 (Fig. 1h). Many of these contacts exhibited bouton-like morphology (Fig. 1h) and co-localized with the presynaptic

marker synaptophysin (Fig. 1h) and vesicular glutamate transporter 1 (vGlut1, Fig. 1h; glutamate is the appropriate neurotransmitter for corticospinal axons) [24]. Synapse formation by regenerating corticospinal axons onto NPC grafts was confirmed by electron microscopy (Fig. 1h). In contrast, lesioned control groups that either received grafts of syngenic bone marrow stromal cells (MSCs) or did not receive any grafts exhibited no corticospinal axon regeneration into the lesion site (Fig. 1i – j, Supplementary Fig. 1). Cell grafts including Schwann cells or MSCs secreting BDNF or NT-3 also failed to support corticospinal regeneration into lesion sites (Supplementary Fig. 1).

Corticospinal axons can regenerate beyond lesion sites

In the T3 transection model, corticospinal axons grew for a maximum distance of 2.5 – 3.0mm into grafts placed in the lesion site (Fig. 1g). To determine whether corticospinal axons could regenerate beyond the lesion site if a smaller lesion/graft was placed, we performed focal CST lesions, without resecting the lateral and ventral portions of the spinal cord, in an effort to limit the rostral-to-cadual length of the lesion cavity and graft. E14 NPCs were placed into this smaller lesion, using a graft cell volume of 1.5 μl (3×10^5 cells) instead of 10 μl (2×10^6 cells) used in the above studies ($n = 6$ rats). When examined six weeks after grafting, four of six animals had small grafts/lesions of ~1.0 mm rostral–to–cadual length, compared to 4.0 –.6.2 mm observed above. In all four of these animals, corticospinal axons crossed the caudal host/graft interface, indicating regeneration beyond the lesion site (Fig. 2a–d). An average of 9.7% of all corticospinal axons quantified 0.5mm rostral to the lesion site crossed the caudal host/graft interface into gray matter but not white matter (Fig. 2e–h).

It is possible that axons crossing the caudal graft/host interface could have arisen from spared ventral or lateral corticospinal axons that were actually entering the graft from the caudal direction, rather than exiting the graft from the rostral direction. However, we did not observe corticospinal axons crossing the caudal graft/host interface in animals with partial lesions but larger grafts, arguing against this possibility (Fig. 3b). Moreover, careful analysis of spared ventral corticospinal axons in very close proximity to the graft demonstrated no instances of axonal penetration into the graft (Fig. 2g), whereas lesioned dorsal corticospinal axons clearly crossed the host/lesion interface to penetrate the graft (Fig. 1a – c, Fig. 2c). Labeling for glial fibrillary acidic protein (GFAP) revealed a significant attenuation of the reactive glial scar surrounding the lesion/graft site ($P < 0.05$; Fig. 2i).

Single-synapse anatomical relays span the lesion

Next, to determine whether regenerating corticospinal axons form connections with grafted neurons that in turn directly project axons to the spinal cord caudal to the lesion site, we injected the retrograde tracer cholera toxin B (CTB) into spinal cord gray matter located two spinal cord segments caudal to the lesion/NPC graft site in four rats, six weeks after C4 CST lesions and NPC grafts (Supplementary Fig. 2a–c). When examined three days after CTB injections, retrogradely-labeled grafted neurons exhibited close appositions with BDA-labeled corticospinal axons in every animal examined (Supplementary Fig. 2d–f). Corticospinal axon terminals on these retrogradely labeled graft neurons expressed vGlut1 (Supplementary Fig. 2g). Quantification revealed that 1.8% of grafted neurons were

retrogradely-labeled with CTB; 26% of these received BDA-labeled corticospinal axon appositions, and 92% of these grafted neurons receiving corticospinal appositions expressed Camk2 (an excitatory neuronal marker; Supplementary Fig. 2h, i).

Regenerating corticospinal axons form functional synapses with grafted neurons

Having established that corticospinal axons regenerate extensively into NPC grafts, we performed additional experiments to further characterize the regenerating axons, and to identify cellular mechanisms associated with regeneration. For these studies, we used spinal level C4 CST lesions in either rat or mouse species; in rats, the corticospinal tract is located within the dorsal columns and contains >98% of all corticospinal axons [5]. The chief advantage of this less extensive lesion model is that animal care is less difficult, and grafts survive and fill the lesion cavity without requiring use of a growth factor cocktail [19] (Fig. 3a), thereby eliminating potentially confounding effects of growth factors in interpreting mechanisms underlying corticospinal regeneration. Nine rats received implants of E14-derived multipotent NPC grafts (2.5μl, 5×10^5 cells) into the C4 CST lesion cavities at the same time that lesions were made. When examined six weeks later, surviving grafts filled the lesion site and supported robust corticospinal regeneration: the number of corticospinal axons quantified at a distance of 0.5mm within the graft represented 72% of the total number of corticospinal axons quantified 0.5mm rostral to the lesion (Fig. 3c). The NPC grafts expressed mature neuronal, glial and oligodendrocyte markers (Fig. 3d, e), as observed in the T3 complete transection model[19].

To assesse whether the synapses formed between regenerating corticospinal axons and neurons in the lesion site (Fig. 1h) were functional, we injected adeno-associated virus-2 (AAV2) vectors expressing channelrhodopsin-2 (ChR2) and GFP into the motor cortex of three adult rats. Two weeks after AAV2 injections, E14 rat multipotent NPC grafts were placed into C4 spinal cord CST lesion sites at the time of injury (Fig. 3f–g). Four weeks after injury and grafting, spinal cord slices were prepared for whole cell recording of optogentically-evoked synaptic responses in grafted neurons. Photic stimulation generated excitatory post-synaptic currents (EPSCs) in three out of 14 graft neurons sampled from two animals (Fig. 3h), and were abolished in the presence of the glutamatergic blocker 6,7-dinitroquinoxaline-2,3-dione (DNQX; 20μM). The presence of functional excitatory synapses was confirmed with a second method, wherein we placed bipolar stimulating electrodes in the main dorsal CST 1mm rostral to the lesion, and performed whole cell recording in graft neurons (Fig. 3i). EPSCs were detected in seven out of 14 graft neurons sampled from three animals (Fig. 3j). These responses were abolished in the presence of DNQX (20μM), confirming that responses were the result of glutamatergic synaptic activation and not a consequence of antidromic activation of graft axons within host tissue or current spread reaching the grafted cells.

Corticospinal regeneration requires an injury signal and contact with the graft

As prior studies have indicated that axotomy primes peripheral neurons to regenerate [25,26], we next examined whether an injury signal was required for corticospinal regeneration. NPC grafts were placed immediately dorsal to and in contact with the CST at the C4 level in 12 rats, without actually transecting the corticospinal projection. Six of these animals then

underwent CST lesions one segment lower than the graft, at C5, while the other six animals underwent sham surgeries without CST lesions (Fig. 4a, b). When assessed six weeks later, corticospinal axon regeneration into grafts was only observed in those animals with transections of the CST (Fig. 4c–g).

To investigate whether regeneration is contact-mediated or generated by diffusible factors from the graft, rats underwent C5 CST lesions and at the same time NPC grafts were placed immediately dorsal to the corticospinal projection one segment higher, at the C4 level. Grafts were placed either in contact with the CST ($n = 5$), or more superficially within 22 – 50 μm of the tract, but not in actual contact with corticospinal axons in the tract ($n = 4$; Fig. 4h). When examined six weeks later, corticospinal axons regenerated into every graft in contact with the tract, but not into any grafts located even a small distance of 22 – 50 μm from the tract (Fig. 4i, j).

Mature grafts support corticospinal regeneration

We hypothesized that only early-stage NPC grafts would enable corticospinal regeneration, since molecules for axon guidance, patterning and differentiation are expressed during developmental stages of the nervous system, and the mature spinal cord is generally considered non-permissive to axonal regeneration [27]. To assess whether the developmental stage of NPCs influences corticospinal regeneration, we characterized the time course of maturation of E14 spinal cord-derived NPCs after *in vivo* grafting into the C4 spinal cord (in the absence of spinal cord lesions) and sacrificed rats 7, 20 and 70 days later ($n = 3$ rats per time point). We found that grafted NPCs predominantly expressed the developmental markers nestin (NPCs) and doublecortin (DCX, immature neurons) one week post-grafting (Supplementary Fig. 3a). A mix of early (nestin, DCX) and mature neuronal markers (NeuN) were evident 20 days post-grafting, and mature markers (neuronal NeuN and oligodendrocyte APC) were exclusively expressed 70 days post-grafting (a time point equivalent to a mature rat; Supplementary Fig. 3a). To assess whether axons can regenerate into mature neural grafts, we took advantage of the observation that corticospinal axons only initiate a regeneration signal when injured. Accordingly, we grafted E14 spinal cord-derived NPCs immediately dorsal to and in contact with the intact CST at C4, and allowed the grafts to mature for 0, 20 or 70 days. C5 CST lesions were then placed at each of these time points ($n = 5$ rats with lesions placed the same day, $n = 4$ rats with lesions at 20 days, and $n = 6$ rats with lesions placed 70 days after grafting, Supplementary Fig. 3b). Analysis of corticospinal regeneration into grafts assessed 6 weeks after lesion revealed that fully mature grafts supported equally robust regeneration compared to immature grafts (Supplementary Fig. 3c – e).

Corticospinal regeneration requires caudalized, homotypic neuronal grafts

Next, we hypothesized that replacement of the spinal cord lesion site with homologous neural tissue was required to support corticospinal regeneration. Accordingly, NPC grafts were prepared from either the spinal cord, hindbrain, or telencephalon of E14 rats and grafted into adult C4 CST lesions ($n = 9$ recipients of spinal cord, $n = 7$ hindbrain, and $n = 7$ telencephalic grafts). We found significant differences in the ability of corticospinal axons to regenerate into grafts isolated from different levels of the neuraxis, with fewer axons

penetrating into grafts of hindbrain than spinal cord, and corticospinal axons largely failing to penetrate telencephalic grafts (Kruskal-Wallis test, $P < 0.01$; Fig. 5a, b). The greatest degree of regeneration occurred into grafts of NPCs derived from the spinal cord ($P < 0.05$, post-hoc Steel-Dwass test compared to hindbrain and $P < 0.01$ compared to telencephalon).

To test the hypothesis that neurons are an essential component of the graft to enable corticospinal regeneration, we prepared neuronal restricted progenitor cells (NRPs) and glial restricted progenitor cells (GRPs) from the developing E12 mouse spinal cord [28]. For this study, we used mice instead of rats because we failed to achieve survival of rat NRPs in lesion sites, as reported previously[29]. Adult mice underwent C4 CST lesions and received implants of either GRPs alone ($n = 9$), a mixture of NRPs/GRPs ($n = 4$), orE12 mouse multipotent NPCs ($n = 9$, Suppl. Fig. 4a–c). When examined six weeks later, grafts of GRPs alone failed to support corticospinal axon regeneration (Supplementary Fig. 4c, d). However, grafts containing a mixture of NRPs/GRPs had surviving neurons and glia, and supported the same degree of corticospinal regeneration as grafts of E12 mouse multipotent NPCs (Supplementary Fig. 4c, d).

NPC grafts improve forelimb function after spinal cord injury

To determine whether NPC grafts influence functional recovery, we performed behavioral assessment on a skilled forelimb reaching task (the staircase task[30]) that is dependent on the motor cortex[31–34] and reflects in part the function of the corticospinal projection[5,30,35]. For this portion of the study, we used bilateral CST lesions plus right dorsal quadrant lesions of the spinal cord, which remove the ipsilateral rubrospinal and lateral corticospinal projections (Supplementary Fig. 5a, b)[36,37]. Adult rats were pre-operatively trained and lesioned, then randomly assigned to receive grafts two weeks later of syngeneic rat E14-derive multipotent NPCs ($n = 9$) or re-exposure of the lesion site without grafting ($n = 9$; Supplementary Fig. 5a–c). One control subject died one week after sham surgery. Two animals were excluded from final analysis because of poor graft survival (Supplementary Figs 5g, h), and one control animal was excluded due to an incomplete lesion that spared the CST. After lesions but prior to grafting, all animals exhibited a severe loss of function on the staircase task (Fig. 5c). After grafting, the treatment group exhibited statistically superior performance compared to control lesioned subjects in overall food pellet retrieval success with the affected forelimb (repeated measures ANOVA $P < 0.05$; post-hoc Fischer's showed significant differences between grafted and lesioned groups beginning five weeks post-grafting; Fig. 5c). Repeated measures ANOVA on two other functional sub-measures of skilled forelimb performance on the staircase task also approached significance, including the most difficult level of the staircase reached ($P = 0.07$) and the percentage of displaced pellets that were eaten ($P = 0.07$). Given the presence and consistency of these trends, we performed exploratory post-hoc analyses that yielded findings consistent with total pellet retrieval: the treatment group separated from the control group beginning about five weeks post-grafting (Fig. 5c).

NPCs do not migrate when grafted into closed lesion cavities

Recent reports indicate that NPCs grafted into open lesion cavities can form ectopic cell colonies [38–41]. This is a safety concern for clinical trials. Among the animals in this study,

we comprehensively assessed whether ectopic cell colonies were present in the neuraxis. A total of 15 rats in this study underwent “open” lesions and grafts, in which the dura is opened and cells are implanted in this open lesion with a fibrin matrix and growth factor cocktail (Supplementary Fig. 6a). Of these 15 animals, six had small ectopic cell deposits. Four were in completely transected animals, and two were in animals with C4 corticospinal/quadrant lesions. These were small groupings of cells located within four spinal segments of the graft site, as described in previous publications (Supplementary Fig. 6b) [39,40]. None of these displaced normal spinal cord tissue. We also examined whether ectopic cell deposits were present in another 78 subjects that underwent grafting into “closed” lesion cavities, without supplemental growth factors. None of these subjects had ectopic cell collections or cell migration within the central canal; migration into the central canal in humans would be unlikely because it is not patent in adults[42].

Human NPC grafts support corticospinal regeneration

To further explore the clinical relevance of NPC grafting in supporting corticospinal axon regeneration, we grafted primary human spinal cord multipotent NPCs isolated from a 9-week old embryo (UCSD1113 line, see Methods) into adult immunodeficient rats[19] that underwent C4 CST lesions ($n = 6$). Corticospinal axons regenerated into human spinal cord-derived NPC grafts when examined six weeks later (Fig. 6a, b). We also grafted human NPCs from the H9 embryonic stem (ES) line [43] into immunodeficient rats using the same experimental paradigm ($n = 9$); these cells express predominantly midbrain markers but not caudal neuraxis markers (Supplementary Fig. 7a, b). We hypothesized that homotypic human spinal cord-derived neural progenitor grafts, but not more rostrally fated neural grafts, would promote corticospinal regeneration. Indeed, corticospinal axons successfully regenerated into spinal cord-derived human grafts and failed to regenerate into rostrally fated human H9 neural cell grafts ($P < 0.01$; Fig. 6a, b). The proportion of cells expressing neuronal markers did not differ when comparing animals that received human spinal cord vs. H9 cell graft types (Supplementary Fig. 7d); the proportion of cells expressing the glial markers GFAP and NG2 at this six week post-implantation time point was less than 1% in both graft types, because human cells require extended time for glial differentiation[44].

We then generated human induced pluripotent stem cells (iPSCs) from skin fibroblasts and drove these toward either rostral (forebrain) or caudal NPC fates without or with the caudalizing morphogen retinoic acid, respectively (Supplementary Fig. 7a, c). NPCs differentiated from iPSCs without the caudalizing morphogen predominantly expressed forebrain neural markers, whereas retinoic acid-treated *i*PSC-derived NPCs predominantly expressed caudal neural markers (Supplementary Fig. 7a, c). Six weeks after grafting to C4 CST lesion sites in immunodeficient rats ($n = 4$ animals per group), corticospinal axons regenerated into human caudalized NPC grafts but not into rostralized grafts ($P < 0.05$; Fig. 6c, d).

DISCUSSION

Recent reports have emphasized the importance of amplifying intrinsic axonal signaling to promote the growth of refractory corticospinal axons after SCI [8,45]. However, these efforts

have not been successful in generating extensive corticospinal regeneration into larger, more clinically relevant lesion sites that lack small bridges of host tissue. We now find that NPC grafts enable the extensive and consistent regeneration of corticospinal axons into sites of severe SCI. Indeed, neural grafts achieve extensive regeneration of corticospinal axons into complete spinal cord transection sites, rather than growth only through spared tissue bridges, an important practical milestone for application to the vast majority of injured humans who have lesion cavitation and relatively little tissue sparing [46]. Successful regeneration does not require therapeutic activation of the corticospinal neuron *per se*; provided solely with a permissive graft milieu, we show for the first time that corticospinal axons are capable of extensive regeneration into a lesion site. The observation that regeneration of corticospinal axons requires actual contact with the graft indicates that growth is likely mediated by ligand-receptor interactions rather than diffusible signals from the graft. This currently unknown ligand-receptor interaction is conserved across species, including humans, since human neural stem cells support rat corticospinal regeneration.

Regenerating corticospinal axons form synapses with grafted neurons that are functional and recapitulate the pre-injured glutamatergic phenotype of the neuron. Regenerating corticospinal synapses form onto grafted neurons that predominantly express CamK2, and some of these neurons in turn extend axons into the caudal spinal cord, thereby establishing potential relays across the lesion site. Electrophysiological measures confirm the presence of excitatory synaptic responses generated by regenerating corticospinal axons within the graft. Corticospinal axons also exhibit an ability to regenerate *beyond* the lesion site and into caudal host gray matter when shorter lesions are placed. This “bridging” regeneration is associated with attenuation of the glial scar at the rostral and caudal host/lesion interfaces, identifying another potential advantage of NPC approaches for neural repair.

Notably, corticospinal regeneration only occurs when NPCs are derived from or driven toward a caudal neural fate, resembling the normal spinal cord target of corticospinal projections. Substitution of the injured spinal cord with neural anlage from other levels of the neuraxis does not support corticospinal regeneration; essentially, *replacement* of the spinal cord enables corticospinal regeneration. Surprisingly, corticospinal regeneration can occur equally well into developing or fully mature grafts, indicating that it is the homotypic nature of the graft to the spinal cord, and not its state of maturity, that supports regeneration. Caudalized human NPC grafts support rodent corticospinal axon regeneration, indicating conservation of cell-cell interactions across species that enable growth of this system. The ability to reconstitute a spinal cord milieu in the lesion site using human neural stem cells derived from ESCs or *i*PSCs, rather than depending on a supply of fresh fetal tissue grafting [47], is an important step toward practicality in translating this technology to humans. The precise molecular constituent(s) of the graft that enable corticospinal regeneration remain to be identified; our findings point toward a graft-specific set of extracellular matrix molecules or cell adhesion molecules. It is also possible that a unique glial sub-type exerts a permissive role in enabling corticospinal regeneration[48].

Having the means in hand to extensively regenerate the corticospinal projection provides an important tool for both future clinical development, and for greater understanding of mechanisms underlying regeneration of what has been the most refractory axonal system

that is critical to human motor function. Practical issues related to clinical translation remain to be addressed, including the identification of the optimal cell type for grafting, and establishment of safe methods for cell engraftment. Recent reports indicate that ectopic stem cell colonies can form after grafting[38_41], although our grafts into closed lesion cavities lacking growth factor cocktails were free of ectopic colonies; additional studies will aim to optimize the grafting technique to minimize the risk of cell spread. Our findings suggest that the use of caudalized neural stem or progenitor cells will be essential for supporting corticospinal regeneration in future translational efforts.

EXPERIMENTAL PROCEDURES

Animals

A total of 248 rats were subjects of this study, including adult female Fischer 344 rats (150–200 g, *n* = 224, Harlan); transgenic Fischer 344 rats expressing GFP ubiquitously, (150–200 g, *n* = 6, Rat Resource and Research Center, University of Missouri, Columbia, MO); and athymic nude rats (150–180 g, *n* = 18, T cell deficient, The Jackson Laboratory, Bar Harbor, ME). A total of 41 mice were used in this study, including C57BL/6 mice (25–35 g, n = 31, The Jackson Laboratory, Bar Harbor, ME); transgenic C57BL/6 GFP mice (25–35 g, n = 10, The Jackson Laboratory, Bar Harbor, ME). NIH guidelines for laboratory animal care and safety were strictly followed. The Institutional Animal Care and Use Committee of the VA San Diego Healthcare System approved all animal surgeries. Animals had free access to food and water throughout the study. All surgery was done under deep anesthesia using a combination (2 ml/kg) of ketamine (25 mg/ml), xylazine (1.3 g/ml), and acepromazine (0.25 mg/ml).

Cell preparation

All cells were prepared and grafted at a concentration of 200,000 cells/μl. Rat multipotent neural progenitor cells (NPCs) were prepared as described previously [49]. Briefly, E14 spinal cord anlage from F344 GFP-expressing transgenic rats were dissociated with 0.05% trypsin and re-suspended in phosphate buffered saline (PBS). For T3 complete transection and C4 right quadrant lesion models, E14-derived spinal cord multipotent NPCs were suspended in a fibrin matrix (25 mg/ml fibrinogen and 25 U/ml thrombin, Sigma) containing a growth factor cocktail to support graft survival as previously described [49]. For grafts of rat NPCs in all other models, cells were re-suspended in PBS. For preparation of mouse multipotent NPCs, we used C57BL/6 mice expressing GFP under the ubiquitin promoter. Mouse E12 spinal cords were dissected and dissociated using the methods described above. Mouse neuronal restricted precursors (NRPs) and glial restricted prescursors (GRPs) were prepared as described previously [50] from E12 GFP mouse spinal cords. On the day of transplantation, cells were dissociated with Accutase (Innovative Cell Technologies, San Diego, CA) and re-suspended in PBS. The human spinal cord neural progenitor cell line UCSD1113 was generated from a 9-week embryonic spinal cord that was dissociated and incubated with TrypLE (Lifetechonologies, Grand Island, NY) for 20 minutes, followed by light mechanical dissociation. Dissociated cells were cultured on plates coated with CELLstart using KnockOut DMEM/F12 culture medium supplemented with 2% of StemPro Neural Supplement (All from Lifetechonologies, Grand Island, NY), 20 ng/ml, FGF2, 20ng/ml

EGF, 10ng/ml LIF, 1% of Glutamax, and 1% penicillin-streptomycin. Cells were expanded to passage 3, dissociated with Acutase, and resuspended in a fibrin matrix containing the growth factor cocktail. Human neural stem cells derived from the H9 embryonic stem cell line were purchased from Life Technologies (Grand Island, NY), and infected overnight with GFP-expressing lentivirus under the CAG promoter. Greater than 97% of the cells expressed GFP in vitro. Human induced pluripotent stem cells (hiPSCs, line IMR90, donated from James Thompson lab at University of Wisconsin-Madison, passage 28–30) were maintained on a feeder layer of irradiated mouse embryonic fibroblasts (MEFs) as described [51,52]. hiPSCs were differentiated to Pax6/Sox1-expressing neuroepithelia (NE) for 10–12 days in a neural induction medium consisting of DMEM/F12, N2 supplement and non-essential amino acids [53]. The neuroepithelial cells formed neural tube-like rosettes at days 10–12 which were gently blown off by a 1-ml pipette on day 15. For generating forebrain NPCs, the spheres were suspended in the same medium. For generating spinal cord neural progenitor cells, retinoic acid (RA, 0.1 μM) was added from days 10–23 to induce a spinal fate [54]. Rat bone marrow stromal cells (MSCs) and primary cultured Schwann cells were prepared and grafted as described previously [55–57]. Cell viability in all grafting experiments was assessed by Trypan blue exclusion (Life Technologies, Grand Island, NY) at the conclusion of the grafting day, and was always within the range of 85% – 98%.

Spinal cord lesions

In this study, we used two lesion models for anatomical study: 1) T3 complete transection, a severe lesion that interrupts all axonal projections across the lesion site, and 2) C4 CST lesions, which remove ~98% of corticospinal projections [58] together with the majority of the dorsal column sensory projection and portions of surrounding gray matter and dorsolateral white matter; these lesions largely spare ventral white and gray matter. C4 CST lesions were used both to simplify animal care, and, importantly, because this lesion allows graft cell survival without use of growth factors that might confound experimental interpretation of mechanisms associated with CST regeneration [59]. To make focal CST lesions, a tungsten wire knife was inserted 1 mm from the dorsal surface of spinal cord and raised 0.8 mm to transect the dorsal corticospinal tract, leaving an overlying remnant of the dorsal column ascending sensory projection, thereby creating an enclosed lesion cavity with intact idura. T3 complete transections were employed to determine whether corticospinal axons are capable of regenerating in this most severe type of spinal cord injury, using previously described methods [49]. For behavior study, we used C4 right quadrant lesions. To place C4 right quadrant lesions, we performed bilateral dorsal column wire knife lesions and right dorsolateral wire knife lesions: the wire knife was inserted into the right dorsal aspect of the spinal cord, 0.5mm from midline. Facing medially, the knife was inserted to a depth of 1mm, the arc of the knife was extruded, and it was raised dorsally toward the spinal cord surface to transect the CST. The wire knife was then retracted and removed from the spinal cord, the knife was rotated 180 degrees to face toward the right lateral side of the spinal cord, and reinserted through the same opening to a depth of 1mm. The blade was then extruded and raised again to the surface of the spinal cord. All animals within an experimental group that underwent lesions were randomly assigned to receive either neural grafts, non-neural grafts or lesion only.

Cell engraftment

In rats with T3 complete transections or C4 right quadrant lesions, NPCs were grafted two weeks after the spinal cord lesion. 10 μl of cells (5 μl in the case of C4 quadrant lesions) were grafted into the lesion cavity through a pulled glass micropipette (OD 80μm) using a PicoSpritzer II (General Valve, Inc., Fairfield, NJ). Subjects were perfused 6 weeks after grafting in T3 lesion subjects and 13 weeks after grafting in C4 right quadrant lesions.

For studies identifying mechanisms that enable rat corticospinal regeneration, 2.5μl of rat NPCs were grafted into C4 CST injury sites immediately after lesions were placed. To study corticospinal axon bridging beyond the lesion, six adult Fisher 344 rats received 1.5 μl of neural progenitor cells, followed by perfusion six weeks later.

To determine whether corticospinal axonal regeneration requires an injury signal, C5 corticospinal tract lesions were placed in adult Fischer 344 rats, and 1μl of E14-derived rat spinal cord neural progenitor cells were grafted into the dorsal column white matter at the C4 level. Cells were micro-injected using an 80μm-OD pulled glass micropipette at a depth of 0.5 mm from dorsal surface of spinal cord. 10 rats received C5 lesions and grafts of neural progenitor cells, and 11 rats received grafts alone without lesions. Any animals in which grafts were inadvertently placed within the corticospinal main tract at C4 were excluded from the analysis, because of the possibility that the graft itself caused an injury to the CST: accordingly, the final numbers of analyzed subjects was 6 per each group.

To investigate whether corticospinal axonal regeneration requires physical contact with NPC grafts, 10 subjects underwent C5 corticospinal tract lesions and, the same day, grafts of E14 spinal cord-derived neural progenitor cells at C4. These grafts were placed with the objective to just make contact with the CST at C4, or to be located slightly dorsal and not in actual physical contact. To be included in analysis, animals had to meet these proximity criteria and grafts could not be located within the corticospinal tract itself at C4. Out of the 15 animals implanted, six subjects were excluded because the graft was located within the corticospinal main tract, or because the graft distance from the tract was more than 50 μm. This left a total of nine subjects in which the graft just made contact with the graft ($n = 5$) or the graft was very close to, but not in contact with, the graft ($n = 4$).

To determine whether grafts of mature NPC grafts can support corticospinal regeneration, adult F344 rats underwent microinjections of rat E14 spinal cord-derived multipotent neural progenitor cell grafts into *intact*, unlesioned C4 dorsal columns at a depth of 0.5mm, aiming for contact with but no lesion of the corticospinal projection. C5 corticospinal tract lesions were then placed either on the same day as grafting ($n = 9$), 20 days after grafting ($n = 8$), or 70 days after grafting ($n = 12$). Additional animals underwent identical grafts to the intact C4 dorsal columns with maturation for 7 days ($n = 3$), 20 days ($n = 5$) or 70 days ($n = 5$), but C5 was never lesioned. In all animals, a total of 1μl of cells were injected into the intact C4 dorsal columns. Subjects in which neural progenitor cells were inadvertently injected directly with the corticospinal tract were excluded from analysis, leaving $n = 5$ animals with grafts and lesions at the same time, $n = 4$ animals with grafts followed by lesions 20 days later, and $n = 6$ animals with grafts and lesions 70 days later. Among animals that received

grafts to the dorsal columns for 0, 20 or 70 days without C5 lesions, $n = 3$ per group per time point met graft placement requirements.

For studies examining whether neurons in grafts were required to enable corticospinal regeneration, C57BL/6 mice were used and C4 corticospinal tract lesions were placed. At the same time as injury, cells were grafted into the lesion site. Nine mice received grafts of glial-restricted precursors (GRPs), and four mice received a mixture of NRPs and GRPs. Nine additional mice received grafts of E12-derived multipotent neural progenitor cells. Six weeks after grafting, all mice were perfused.

For human neural stem cell grafting studies, C4 corticospinal lesions were placed in adult immunodeficient rats. Two weeks later, 2.5μl suspensions of human multipotent NPCs from embryonic spinal cord ($n = 6$), human H9 ES-derived neural stem cells ($n = 9$), rostralized human iPSC-derived neural stem cells ($n = 4$) or caudalized human iPSC-derived neural stem cells ($n = 4$) were injected into the lesion site, followed by perfusion 6 weeks later.

For anatomical MSCs or Schwann cell transplantation studies, female adult Fisher rats underwent 2.5 μl of cell suspension graft of MSCs-GFP ($n = 6$), MSCs-NT3-GFP ($n = 6$), MSCs-BDNF-GFP ($n = 6$), and Schwann cells ($n = 6$) into C4 CST lesion at the same time of injury, followed by perfusion 6 weeks later.

Electrophysiology

To examine synaptic function between regenerating corticospinal axons and neural grafts, three rats received 16 injections of AAV2-CAG-channel rhodopsin-2 - GFP (ChR2-GFP, 6 μl, 1.0×10^{12} particles per ml, UNC Vector Core, Chapel Hill, NC) into bilateral motor cortices at coordinates described previously [58]. Two weeks later, C4 corticospinal tract lesions were placed and neural progenitor cells were grafted into the lesion site. Four weeks later, animals were transcardially perfused for 3 min with ice-cold, oxygenated, modified sucrose artificial cerebrospinal fluid (ACSF) containing (in mM) 75 NaCl, 2.5 KCl, 3.3 MgSO4, 0.5 CaCl2, 1NaH2PO4, 26.2 NaHCO3, 22 glucose, 52.6 sucrose, 10 HEPES, 10 choline chloride, 1 pyruvate and 1 L-ascorbic acid (~300 mOsml, pH 7.4). A 1.5 cm-long section of the spinal cord containing the graft was rapidly dissected and the dura was removed. The cord was mounted onto an agarose block and sagittal slices (330 μm) were cut and collected in ice-cold, oxygenated, modified sucrose ACSF. Slices were transferred to an interface chamber containing the same modified sucrose ACSF solution and incubated at 34° C for 30 min. Slices were held at room temperature (23° C) in the interface chamber for at least 45 min before initiating recordings. Recordings were made in a submersion-type recording chamber and perfused with oxygenated ACSF containing (in mM) 119 NaCl, 2.5 KCl, 1.3 MgCl2, 2.5 CaCl2, 1.3 NaH2PO4, 26.0 NaHCO3, 20 glucose (~300 mOsml) at 23° C at a rate of 2–3 ml/minute. RFP expressing grafts were initially identified by their fluorescent emission spectra and were then targeted for whole cell recording under infrared differential interference contrast videomicroscopy (Olympus BX-51 scope and Rolera XR digital camera). Whole-cell patch clamp recordings were obtained using Multiclamp 700B patch amplifiers (Molecular Devices) and data analyzed using pClamp 10 software (Molecular Devices). Voltage and current clamp recordings were made at room temperature using pulled patch pipettes (4–7 MΩ) filled with internal solution containing (in mM) 150

K-Gluconate, 1.5 MgCl2, 5.0 HEPES, 1 EGTA, 10 phosphocreatine, 2.0 ATP, and 0.3 GTP. To stimulate corticospinal axons, graft containing slices were exposed to a 5 ms pulse of 470 nm light (delivered by an LED; Thor Labs), or extracellular bipolar electrodes (500 μm interelectrode spacing) were placed in the corticospinal tract 1 mm above the graft. Post-synaptic responses were analyzed exclusively from graft cells with a resting membrane potential ≤ −55mV, with drift less than 6 mV over the entire recording period, with access resistance ≤ 35 MΩ, and with the ability to evoke multiple spikes with >60 mV peak amplitude from threshold.

Anterograde and Retrograde Tracing

To trace corticospinal axons in rats, 5μl of 10% BDA (MW 10,000, Lifetechonologies, Grand Island, NY) was injected into 8 sites per hemisphere into bilateral motor cortices two weeks before perfusion [58]. In mice, 2.5 μl of BDA were injected into 5 sites per hemisphere [60].

Retrograde labeling of graft neurons extending axons to caudal spinal cord segments was conducted by injecting 1μl cholera toxin B (CTB; 1% solution; List biological Laboratories, Campbell CA) into bilateral C6/7 spinal gray matter in four Fischer 344 rats that had undergone C4 corticospinal tract lesions and grafts of neural progenitor cells into the lesion site. CTB was injected 6 weeks after lesion/grafting, and animals were perfused 3d later.

Histology and Immunohistochemistry

Spinal cords with T3 complete transections and grafts were horizontally sectioned on a cryostat at 30 μm intervals. All other spinal cords containing the lesion/graft site were sagittally sectioned at 30μm intervals. Sections were incubated with primary antibodies against GFP (rabbit from Invitrogen at 1:1000 or chicken from Abcam at 1:1000); GFAP (mouse from Chemicon at 1:1000 or rabbit from Dako at 1:750 to label astrocytes); human GFAP (rabbit from Origene at 1:500 to label human specific astrocytes); NeuN (mouse from Chemicon at 1:500 to label mature neurons); ChAT (goat from Chemicon at 1:250 to label spinal cord motor neurons); MAP2 (mouse from Chemicon at 1:2,000 to label dendrites); vesicular glutamate transporters 1 (vGlut1, mouse from Chemicon at 1:1,000 to label glutamatergic terminals); synaptophysin (mouse from Chemicon at 1:1,000 to label presynaptic terminals); adenomatous polyposis coli (APC, mouse from Oncogene at 1:400 to label oligodendrocytes); NG2 (rabbit from Millipore at 1:400 to label oligodendrocyte precursors); Hu (human at 1:1000 to label neurons, generous gift from Robert Darnell, The Rockefeller University, NY); doublecortin (DCX, goat from Santa Cruz at 1: 250 to label immature neurons); nestin (mouse from BD at 1:200 to label neural progenitor cells); neurofilament (NF200; mouse from Millipore at 1:250 to label axons); 27C7 (mouse at 1:200 to label Schwann cells, generous gift from K. Wewetzer, University of Freiburg, Freiburg, Germanyat); RFP (mouse from Abcam at 1:200); human nuclei (mouse from Millipore at 1:200); PAX6 (rabbit from Covance at 1:1000); Pax6 (mouse from DHSB at 1:5000); Sox1 (Goat from R&B at 1:1000); HoxB4 (Rat from DHSB at 1:50); FoxG1 (rabbit from Abcam at 1:100); OTX2 (goat from R and D at 1:2000); EN1 (mouse from DHSB at 1:800); Camk2 (rabbit from Genetex at 1:200), and Dyelight 405 or 594-conjugated streptavidin (from Invitrogen at 1:250 to label BDA traced CST axons). Then, sections were

incubated in Alexa 488, 594, or 647 conjugated goat or donkey secondary antibodies (1:500, Invitrogen) for 2.5 hr at room temperature. For nuclear staining, 4′,6-diamidino-2-phenylindole (DAPI, 200 ng/ml) was added to the final wash. Electron microscopic analysis of synapse formation was performed as published previously [49].

Quantification of corticospinal axons

The number of corticospinal axons regenerating into grafts in lesion sites was quantified using StereoInvestigator (MicroBrightField, http://www.mbfbioscience.com) as previously described [49,61]. Briefly, 1-in-6 sections were stained for BDA-labeled CST axons. Dorsal-to-ventral virtual lines were placed at 100× magnification, and then examined under 400× magnification. BDA-labeled axons that intersected the line were marked and counted. In the T3 complete transection model, all sections were used for quantification. In the C4 dorsal column lesion model, two sagittal sections containing the heaviest density of corticospinal main tract axons were quantified using the same methods. In some experiments, we also measured the density of corticospinal axons in grafts (Fig. 3, Suppl. Fig. 3) as described previously [61]. Using the same method, the density of the main CST itself, outside the graft, was also quantified, and the density of corticospinal axons in the graft relative to the main tract was calculated. All measurements were performed with examiner blinded to group identity.

Quantification of glial scar

Fluorescently immunolabeled sections for GFAP and GFP were used to quantify percentage of field occupied by GFAP immunoreactivity surrounding the graft/lesion cavity or lesion cavity alone, as previously described [62]. A 100μm-wide zone surrounding the lesion site was quantified in this manner.

Quantification of cell types in grafts

To quantify neuronal differentiation in E14 rat NPC grafts, fluorescently immunolabeled sections for NeuN, GFAP, APC, GFP, and DAPI were used. Using confocal microscopy (Olympus FV-1000), a minimum of 500 cells per graft were sampled in images (600× mangification) from randomly selected regions of grafts. The proportion of neural marker expressing cells to total number of DAPI was then calculated and averaged among groups. For quantification of neural differentiation in human cell grafts, Hu, human GFAP, NG2 and human nuclei were used. Using the same method described above, the proportion of neural marker-expressing cells to total human cell number was calculated and averaged among groups.

Behavioral studies

18 adult female Fisher rats were trained on the staircase task for three weeks prior to undergoing C4 right quadrant lesions. The staircase task (Lafayette Instrument Company; Lafayette, IN) was performed as described previously [63]. Briefly, rats were allowed 15 min to consume sugar pellets *ad libitum* while in the apparatus. Investigators blinded to group identity recorded the number of pellets displaced, eaten, or dropped, and the deepest stair level reached. Pellet retrieval accuracy was calculated as percentage of sugar pellets

displaced that were eaten. All subjects underwent weekly post-grafting functional testing until the end of the behavioral testing period.

Quantitative reverse transcription-polymerase chain reaction (RT-PCR)

Total RNA was isolated from neural progenitor cell cultures using the RNeasy Mini kit (Qiagen, Germantown, PA) following the manufacturer's protocol. Human fetal whole brain and spinal cord RNAs were purchased from Clontech (Mountain View, CA) and used as controls. For cDNA synthesis, the reverse transcription reaction was performed using the PrimeScript™ RT Master Mix (Perfect Real Time, Clonthech) and quantitative PCR was performed using primers listed in Supplementary Table 1 and SYBR® Premix Ex Taq™ II (Tli RNase H Plus, Clontech) in 20-μL reactions. Data were normalized to glyceraldehydes-3-phosphate dehydrogenase expression (GAPDH).

Statistical Analysis

Multiple group comparisons were made by Kruskal-Wallis ANOVA with Steel-Dwass test (Fig. 5b, , Suppl. Fig. 3e, d, H, Suppl. Fig. 4b) or repeated measures ANOVA (Fig. 5c, Suppl. Fig. 7d) or. Two group comparison was made using the Wilcoxon test (Fig. 2i, Fig. 4g, j and Fig. 6b, d). Normality of data was assessed using the Shapiro-Wilk test. All statistics were performed by JMP software (SAS, Cary, NC) with a designated significance level of 95%. Data are presented as mean ±SEM. As stated above, observers were blinded to group identity while performing all quantifications.

Supplementary Material

Refer to Web version on PubMed Central for supplementary material.

Acknowledgments

We thank Lori Graham, Yaozhi Yang, Eileen Boehle, Janet K Lee, MinJae Kim, Evelyn Liu, Rand Pope, Hans Strobl, and Tre Moynihan for technical assistance; Planned Parenthood; the Rat Resource and Research Center, University of Missouri, Columbia, MO, for providing GFP rats; K. Wewetzer, University of Freiburg, Germany, for providing 27C7 antibody; Robert Darnell, The Rockefeller University, NY, for providing Hu antibody; Ying Jones for use of the electron microscopy core facility at Cellular and Molecular Medicine, University of California, San Diego; and Nikon Imaging Center at Hokkaido University for use of the confocal laser microscopy. This work was supported by the Veterans Administration (Gordon Mansfield Spinal Cord Injury Consortium, M.T. P.L.), the NIH (NS042291; M.T), The Craig H. Neilsen Foundation (K.K., H.K., and J.D.), the Bernard and Anne Spitzer Charitable Trust (M.T.), the Dr. Miriam and Sheldon G. Adelson Medical Research Foundation (M.T. and J.C.), Kobayashi Hospital Furate Research Fund (K.K), Japan Society for the Promotion of Science (H, K.), and the Busta Family and Bleser Family funds (S.C.Z.).

References

1. Liu K, Tedeschi A, Park KK, He Z. Neuronal intrinsic mechanisms of axon regeneration. Annu Rev Neurosci. 2011; 34:131–152. [PubMed: 21438684]
2. Tuszynski MH, Steward O. Concepts and methods for the study of axonal regeneration in the CNS. Neuron. 2012; 74:777–791. [PubMed: 22681683]
3. Bareyre FM, et al. The injured spinal cord spontaneously forms a new intraspinal circuit in adult rats. Nat Neurosci. 2004; 7:269–277. [PubMed: 14966523]
4. Rosenzweig ES, et al. Extensive spontaneous plasticity of corticospinal projections after primate spinal cord injury. Nat Neurosci. 2010; 13:1505–1510. [PubMed: 21076427]

5. Weidner N, Ner A, Salimi N, Tuszynski MH. Spontaneous corticospinal axonal plasticity and functional recovery after adult central nervous system injury. Proc Natl Acad Sci U S A. 2001; 98:3513–3518. [PubMed: 11248109]
6. Schnell L, Schwab ME. Axonal regeneration in the rat spinal cord produced by an antibody against myelin-associated neurite growth inhibitors. Nature. 1990; 343:269–272. [PubMed: 2300171]
7. GrandPre T, Li S, Strittmatter SM. Nogo-66 receptor antagonist peptide promotes axonal regeneration. Nature. 2002; 417:547–551. [PubMed: 12037567]
8. Liu K, et al. PTEN deletion enhances the regenerative ability of adult corticospinal neurons. Nat Neurosci. 2010; 13:1075–1081. [PubMed: 20694004]
9. Zukor K, et al. Short hairpin RNA against PTEN enhances regenerative growth of corticospinal tract axons after spinal cord injury. J Neurosci. 2013; 33:15350–15361. [PubMed: 24068802]
10. Ohtake Y, et al. The effect of systemic PTEN antagonist peptides on axon growth and functional recovery after spinal cord injury. Biomaterials. 2014; 35:4610–4626. [PubMed: 24630093]
11. Starkey ML, Schwab ME. Anti-Nogo-A and training: can one plus one equal three? Exp Neurol. 2012; 235:53–61. [PubMed: 21530508]
12. Hollis ER 2nd, Jamshidi P, Low K, Blesch A, Tuszynski MH. Induction of corticospinal regeneration by lentiviral trkB-induced Erk activation. Proc Natl Acad Sci U S A. 2009; 106:7215–7220. [PubMed: 19359495]
13. Xu XM, Guenard V, Kleitman N, Aebischer P, Bunge MB. A combination of BDNF and NT-3 promotes supraspinal axonal regeneration into Schwann cell grafts in adult rat thoracic spinal cord. Exp Neurol. 1995; 134:261–272. [PubMed: 7556546]
14. Vavrek R, Pearse DD, Fouad K. Neuronal populations capable of regeneration following a combined treatment in rats with spinal cord transection. J Neurotrauma. 2007; 24:1667–1673. [PubMed: 17970629]
15. Lu P, et al. Motor axonal regeneration after partial and complete spinal cord transection. J Neurosci. 2012; 32:8208–8218. [PubMed: 22699902]
16. Lee YS, et al. Nerve regeneration restores supraspinal control of bladder function after complete spinal cord injury. J Neurosci. 2013; 33:10591–10606. [PubMed: 23804083]
17. Cummings BJ, et al. Human neural stem cells differentiate and promote locomotor recovery in spinal cord-injured mice. Proc Natl Acad Sci U S A. 2005; 102:14069–14074. [PubMed: 16172374]
18. Bonner JF, et al. Grafted neural progenitors integrate and restore synaptic connectivity across the injured spinal cord. J Neurosci. 2011; 31:4675–4686. [PubMed: 21430166]
19. Lu P, et al. Long-distance growth and connectivity of neural stem cells after severe spinal cord injury. Cell. 2012; 150:1264–1273. [PubMed: 22980985]
20. Lu P, et al. Long-distance axonal growth from human induced pluripotent stem cells after spinal cord injury. Neuron. 2014; 83:789–796. [PubMed: 25123310]
21. Peljto M, Dasen JS, Mazzoni EO, Jessell TM, Wichterle H. Functional diversity of ESC-derived motor neuron subtypes revealed through intraspinal transplantation. Cell stem cell. 2010; 7:355–366. [PubMed: 20804971]
22. Ma L, et al. Human embryonic stem cell-derived GABA neurons correct locomotion deficits in quinolinic acid-lesioned mice. Cell stem cell. 2012; 10:455–464. [PubMed: 22424902]
23. Mayer-Proschel M, Kalyani AJ, Mujtaba T, Rao MS. Isolation of lineage-restricted neuronal precursors from multipotent neuroepithelial stem cells. Neuron. 1997; 19:773–785. [PubMed: 9354325]
24. Du Beau A, et al. Neurotransmitter phenotypes of descending systems in the rat lumbar spinal cord. Neuroscience. 2012; 227:67–79. [PubMed: 23018001]
25. Perry RB, et al. Subcellular knockout of importin beta1 perturbs axonal retrograde signaling. Neuron. 2012; 75:294–305. [PubMed: 22841314]
26. Cho Y, Sloutsky R, Naegle KM, Cavalli V. Injury-induced HDAC5 nuclear export is essential for axon regeneration. Cell. 2013; 155:894–908. [PubMed: 24209626]
27. Fawcett JW, Schwab ME, Montani L, Brazda N, Muller HW. Defeating inhibition of regeneration by scar and myelin components. Handb Clin Neurol. 2012; 109:503–522. [PubMed: 23098733]

28. Liu Y, Rao MS. Glial progenitors in the CNS and possible lineage relationships among them. Biol Cell. 2004; 96:279–290. [PubMed: 15145532]
29. Cao QL, Howard RM, Dennison JB, Whittemore SR. Differentiation of engrafted neuronal-restricted precursor cells is inhibited in the traumatically injured spinal cord. Exp Neurol. 2002; 177:349–359. [PubMed: 12429182]
30. Garcia-Alias G, Barkhuysen S, Buckle M, Fawcett JW. Chondroitinase ABC treatment opens a window of opportunity for task-specific rehabilitation. Nat Neurosci. 2009; 12:1145–1151. [PubMed: 19668200]
31. Conner JM, Chiba AA, Tuszynski MH. The basal forebrain cholinergic system is essential for cortical plasticity and functional recovery following brain injury. Neuron. 2005; 46:173–179. [PubMed: 15848797]
32. Montoya CP, Campbell-Hope LJ, Pemberton KD, Dunnett SB. The “staircase test”: a measure of independent forelimb reaching and grasping abilities in rats. Journal of neuroscience methods. 1991; 36:219–228. [PubMed: 2062117]
33. Wahl AS, et al. Neuronal repair. Asynchronous therapy restores motor control by rewiring of the rat corticospinal tract after stroke. Science. 2014; 344:1250–1255. [PubMed: 24926013]
34. Alaverdashvili M, Whishaw IQ. Motor cortex stroke impairs individual digit movement in skilled reaching by the rat. Eur J Neurosci. 2008; 28:311–322. [PubMed: 18702702]
35. Whishaw IQ, Gorny B, Sarna J. Paw and limb use in skilled and spontaneous reaching after pyramidal tract, red nucleus and combined lesions in the rat: behavioral and anatomical dissociations. Behav Brain Res. 1998; 93:167–183. [PubMed: 9659998]
36. Girgis J, et al. Reaching training in rats with spinal cord injury promotes plasticity and task specific recovery. Brain. 2007; 130:2993–3003. [PubMed: 17928316]
37. Krajacic A, Weishaupt N, Girgis J, Tetzlaff W, Fouad K. Training-induced plasticity in rats with cervical spinal cord injury: effects and side effects. Behav Brain Res. 2010; 214:323–331. [PubMed: 20573587]
38. Steward O, Sharp KG, Matsudaira Yee K. Long-distance migration and colonization of transplanted neural stem cells. Cell. 2014; 156:385–387. [PubMed: 24485444]
39. Tuszynski MH, et al. Neural stem cell dissemination after grafting to CNS injury sites. Cell. 2014; 156:388–389. [PubMed: 24485445]
40. Tuszynski MH, et al. Neural stem cells in models of spinal cord injury. Exp Neurol. 2014; 261:494–500. [PubMed: 25079369]
41. Steward O, Sharp KG, Yee KM, Hatch MN, Bonner JF. Characterization of ectopic colonies that form in widespread areas of the nervous system with neural stem cell transplants into the site of a severe spinal cord injury. J Neurosci. 2014; 34:14013–14021. [PubMed: 25319698]
42. Garcia-Ovejero D, et al. The ependymal region of the adult human spinal cord differs from other species and shows ependymoma-like features. Brain. 2015; 138:1583–1597. [PubMed: 25882650]
43. Conti L, Cattaneo E. Neural stem cell systems: physiological players or in vitro entities? Nat Rev Neurosci. 2010; 11:176–187. [PubMed: 20107441]
44. Chen H, et al. Human-derived neural progenitors functionally replace astrocytes in adult mice. J Clin Invest. 2015; 125:1033–1042. [PubMed: 25642771]
45. Blackmore MG, et al. Kruppel-like Factor 7 engineered for transcriptional activation promotes axon regeneration in the adult corticospinal tract. Proc Natl Acad Sci U S A. 2012; 109:7517–7522. [PubMed: 22529377]
46. Norenberg MD, Smith J, Marcillo A. The pathology of human spinal cord injury: defining the problems. J Neurotrauma. 2004; 21:429–440. [PubMed: 15115592]
47. Coumans JV, et al. Axonal regeneration and functional recovery after complete spinal cord transection in rats by delayed treatment with transplants and neurotrophins. J Neurosci. 2001; 21:9334–9344. [PubMed: 11717367]
48. Molofsky AV, et al. Astrocyte-encoded positional cues maintain sensorimotor circuit integrity. Nature. 2014; 509:189–194. [PubMed: 24776795]
49. Lu P, et al. Long-distance growth and connectivity of neural stem cells after severe spinal cord injury. Cell. 2012; 150:1264–1273. [PubMed: 22980985]

50. Wu Y, Liu Y, Chesnut JD, Rao MS. Isolation of neural stem and precursor cells from rodent tissue. Methods Mol Biol. 2008; 438:39–53. [PubMed: 18369748]
51. Thomson JA, et al. Embryonic stem cell lines derived from human blastocysts. Science. 1998; 282:1145–1147. [PubMed: 9804556]
52. Yu J, et al. Induced pluripotent stem cell lines derived from human somatic cells. Science. 2007; 318:1917–1920. [PubMed: 18029452]
53. Zhang SC, Wernig M, Duncan ID, Brustle O, Thomson JA. In vitro differentiation of transplantable neural precursors from human embryonic stem cells. Nature biotechnology. 2001; 19:1129–1133.
54. Hu BY, Zhang SC. Differentiation of spinal motor neurons from pluripotent human stem cells. Nat Protoc. 2009; 4:1295–1304. [PubMed: 19696748]
55. Weidner N, Blesch A, Grill RJ, Tuszynski MH. Nerve growth factor-hypersecreting Schwann cell grafts augment and guide spinal cord axonal growth and remyelinate central nervous system axons in a phenotypically appropriate manner that correlates with expression of L1. J Comp Neurol. 1999; 413:495–506. [PubMed: 10495438]
56. Kadoya K, et al. Combined intrinsic and extrinsic neuronal mechanisms facilitate bridging axonal regeneration one year after spinal cord injury. Neuron. 2009; 64:165–172. [PubMed: 19874785]
57. Lu P, et al. Motor axonal regeneration after partial and complete spinal cord transection. J Neurosci. 2012; 32:8208–8218. [PubMed: 22699902]
58. Weidner N, Ner A, Salimi N, Tuszynski MH. Spontaneous corticospinal axonal plasticity and functional recovery after adult central nervous system injury. Proc Natl Acad Sci U S A. 2001; 98:3513–3518. [PubMed: 11248109]
59. Tuszynski MH, Steward O. Concepts and methods for the study of axonal regeneration in the CNS. Neuron. 2012; 74:777–791. [PubMed: 22681683]
60. Liu K, et al. PTEN deletion enhances the regenerative ability of adult corticospinal neurons. Nat Neurosci. 2010; 13:1075–1081. [PubMed: 20694004]
61. Rosenzweig ES, et al. Extensive spontaneous plasticity of corticospinal projections after primate spinal cord injury. Nat Neurosci. 2010; 13:1505–1510. [PubMed: 21076427]
62. Jones LL, Tuszynski MH. Spinal cord injury elicits expression of keratan sulfate proteoglycans by macrophages, reactive microglia, and oligodendrocyte progenitors. J Neurosci. 2002; 22:4611–4624. [PubMed: 12040068]
63. Wang D, Ichiyama RM, Zhao R, Andrews MR, Fawcett JW. Chondroitinase combined with rehabilitation promotes recovery of forelimb function in rats with chronic spinal cord injury. J Neurosci. 2011; 31:9332–9344. [PubMed: 21697383]

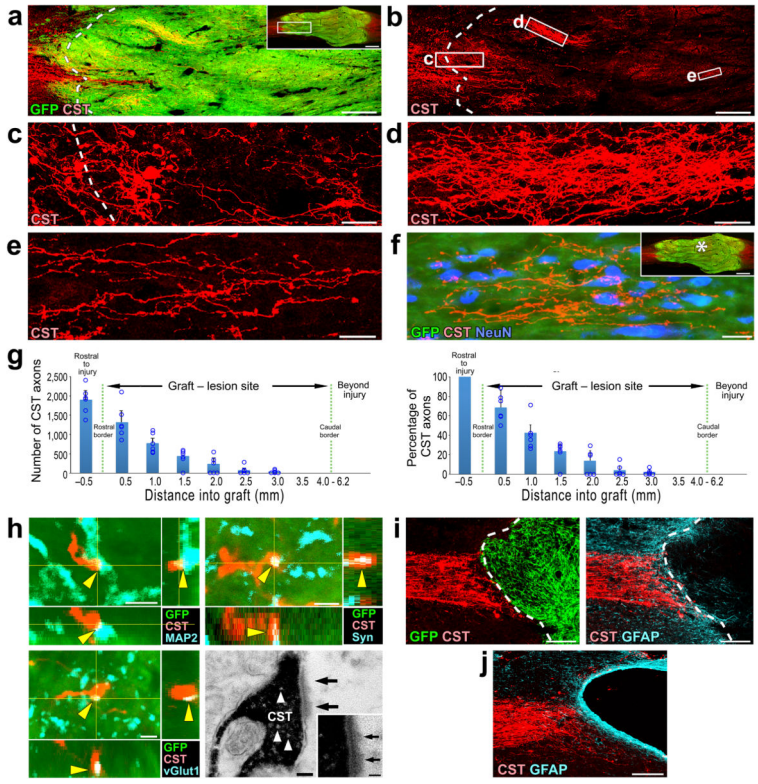

Figure 1. Corticospinal axons extensively regenerate into NPC grafts

(**a**–**b**) Rostral aspect of a GFP-expressing multipotent NPC graft in the site of T3 complete spinal cord transection, shown in horizontal section. Rostral is left, caudal is right. CST axons are labeled with biotinylated dextran amine (BDA, shown in red). Inset shows overview of the graft. Scale bar, 240 μm; 1 mm (inset). (**b**) The CST approaches and regenerates into an NPC graft in the lesion site. Scale bar, 240 μm. (**c**–**e**) Higher magnification views of boxed areas in **b** show the density, varicosities, and tortuosities of regenerating corticospinal axons that extend into the graft. Scale bars **c,** 60 μm; **d,** 30 μm; **e**, 20 μm. (**f**) Regenerating CST axons surround neurons in the center of the graft (* in the inset), 3mm from the rostral host–graft border. Inset shows overview of the graft. Scale bar, 20 μm; 1 mm (inset). (**g**) Quantification of CST axons in NPC grafts in six rats (left). Quantification of the proportion of CST axons in NPC grafts, normalized to the total number of CST axons 0.5mm rostral to the lesion site in six rats (right). Data are presented as mean ± SEM. Circles indicate data from individual rats. (**h**) Triple labeling for GFP, CST, and microtubule-associated protein 2 (MAP2) demonstrates a CST axon in the graft that exhibits a bouton-like swelling in close apposition to a dendrite of a grafted neuron, labeled with MAP2 (arrowheads; upper left, scale bar, 2 μm). Triple labeling for GFP, CST, and synaptophysin (Syn; upper right, scale bar, 2 μm) or vesicular glutamate transporter 1 (vGlut1; lower left, scale bar, 2 μm) in the graft indicates that the corticospinal axon in the graft is co-localized with presynaptic and excitatory synaptic markers, respectively (arrowheads). Electron microscopy image of a 3,3′-diaminobenzidine (DAB)–labeled CST axon terminal (black) forming a synapse (arrows) with a neuronal process within the graft (lower right). Arrowheads indicate presynaptic vesicles. Scale bar, 100 nm. (**i**) Sagittal

images of GPF-expressing syngenic bone marrow stromal cell (MSC) grafts in the site of C4 spinal cord transection. Left, double labeling for CST axons (red) and GFP expressing MSCs (green); right, double labeling for CST axons and glial fibrillary acidic protein (GFAP, blue). Dashed lines indicate rostral host/graft interface. Scale bar, 200 μm. (**j**) Sagittal image of CST axons in a C4 CST transection lesion in the absence of any graft. Scale bar, 200 μm.

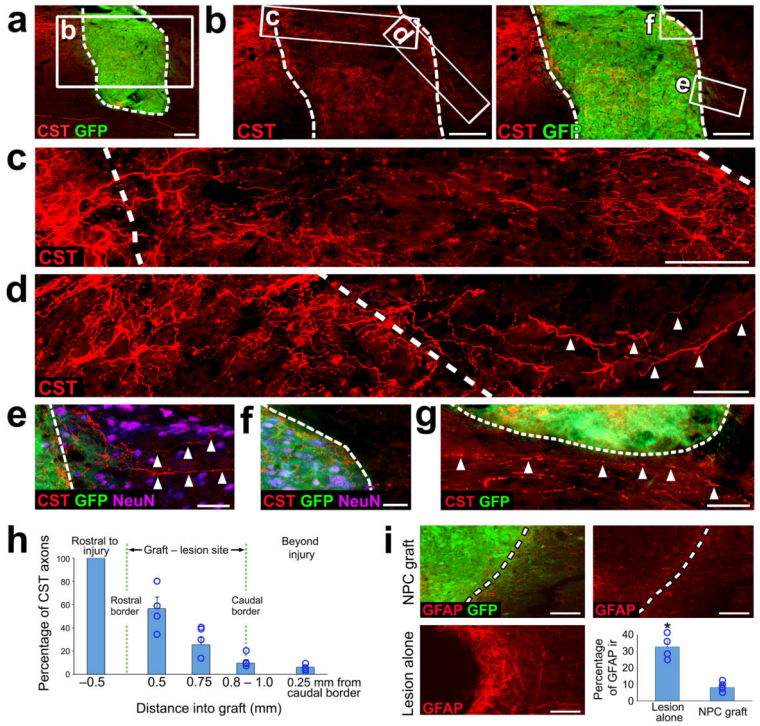

Figure 2. Axonal regeneration beyond the graft in focal CST lesions

(**a**) Low magnification sagittal overview of CST axons (red) and a rat E14 spinal cord NPC graft (green) placed at the focal CST lesion site six weeks after injury. Scale bar, 200 μm. Dashed lines indicate host/graft interface throughout. Rostral is to the left throughout. (**b**) High magnification views of boxed area in **a**. Scale bar, 200 μm. (**c**) High magnification view of boxed area in **b** including rostral host/graft interface. Scale bar, 100 μm. (**d**) High magnification view of boxed area in **b**. Arrowheads indicate CST axons extending beyond the caudal host/graft interface. Scale bar, 50 μm. (**e**–**f**) High magnification views of the boxed areas in **b**. Arrowheads indicate CST axons penetrating host gray matter (**f**, NeuN-positive) but not white matter (**g**, NeuN-negative) caudal to the graft/lesion site. Scale bars, **e**, 50 μm; **f**, 100 μm. (**g**) High magnification view of the area just ventral to the graft/lesion site. Arrowheads indicate spared ventral CST axons located close to the NPC graft. Scale bar, 50 μm. (**h**) Quantification of the proportion of regenerating CST axons found at different locations across the rostro-caudal axis of the NPC graft (n = 4 rats). (**j**) Example images of GFAP immunoreactivity in the vicinity of the host/graft interface of focal CST lesioned rats after receiving (top images) or not receiving (lower left) NPC graft. Scale bars, 100 μm. Quantification of GFAP immunoreactivity at the lesion boundary (n = 4 rats lesion alone, n = 4 rats NPC graft). Throughout, error bars represent mean ± s.e.m. Circles indicate data from individual rats. *P<0.05; Wilcoxon test.

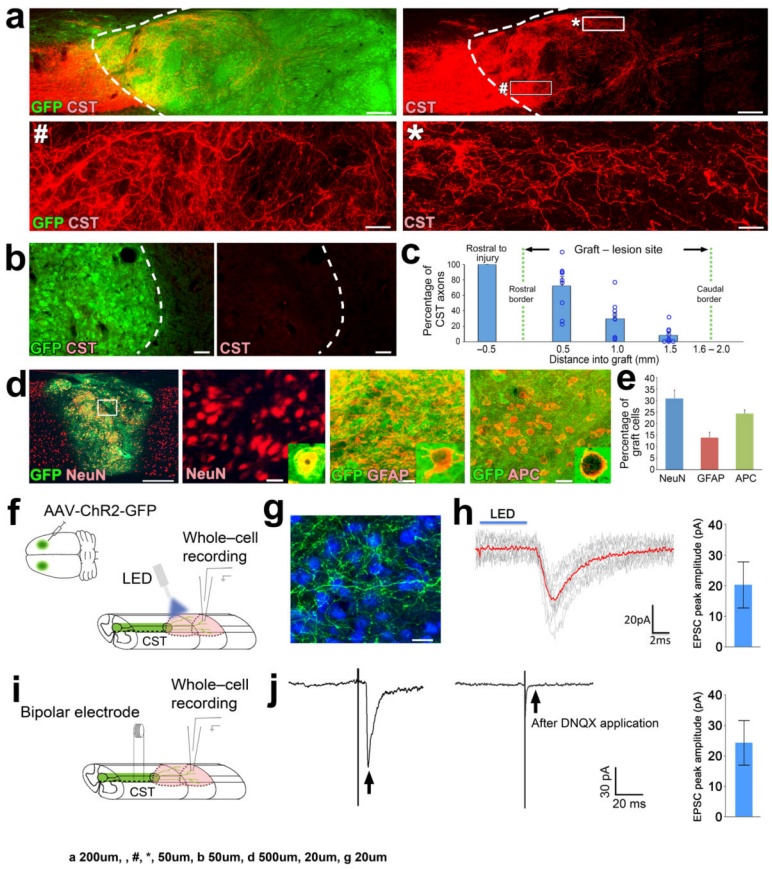

Figure 3. Electrophysiological connectivity between regenerating corticospinal axons and grafted neurons

(**a**) Sagittal views of CST axons (red) and GFP-expressing NPC grafts (green) placed in C4 CST lesions in rats six weeks after injury. Dashed lines indicate rostral host/graft border. Rostral is to the left throughout. Lower panels are high magnification views of boxed areas in upper right panel. Scale bars, 200 μm (upper panels); 50 μm (lower panels). (**b**) Sagittal views of the caudal graft/host interface (dashed lines) in a C4 CST lesioned rat depicting CST axons (red) and GFP-expressing NPC grafts (green). Scale bars, 50 μm. (**c**) Quantification of the proportion of regenerating CST axons (normalized to the total number of CST axons 0.5mm rostral to the graft/lesion site) found at different locations across the rostro-caudal axis of the NPC graft (n = 9 rats). Circles indicate data from individual rats. **(d)** Double immunolabeling of GFP-labeled NPC grafts (green) with neuronal (NeuN, red), astrocytic (GFAP, red) and mature oligodendrocytic (adenomatous polyposis coli, APC, red) cell type markers. Boxed region in the low magnification image on the left is shown at higher magnification immediately to the right. Scale bars, 500 μm (left); 20 μm (all panels to the right). (**e**) Quantification of cell type marker immunoreactivity in grafts. (**f**) Experimental paradigm to record optogenetically-evoked synaptic responses. AAV2 vectors expressing ChR2 and GFP were injected into motor cortices, followed by NPCs grafts into lesion cavities two weeks later. Four weeks after NPC grafts, ChR2+ CST axons were stimulated with blue light (n = 3 rats) and whole-cell recordings of grafted neurons were performed. (**g**) Double immunolabeling for CST axons (green) and neurons (NeuN, blue). Scale bar, 20 μm.

(**h**) EPSCs recorded from a grafted neuron evoked with 5 ms of 470 nm light (blue line). Red trace indicates the average of individual EPSCs (gray traces). Averaged peak EPSC amplitude from three responding cells is plotted to the right (**i**) Experimental paradigm to record electrically-evoked synaptic responses. During whole-cell recordings of grafted neurons, CST axons were stimulated by bipolar electrodes positioned 1mm rostral to graft. (**j**) Example of an evoked EPSC (arrow, left) recorded from a grafted neuron. Application of the AMPAR antagonist DNQX (20μM) abolished responses (arrow, right), indicative of a glutamatergic synapse. Averaged peak EPSC amplitude from seven responding cells is plotted to the right. Error bars represent mean ± s.e.m throughout.

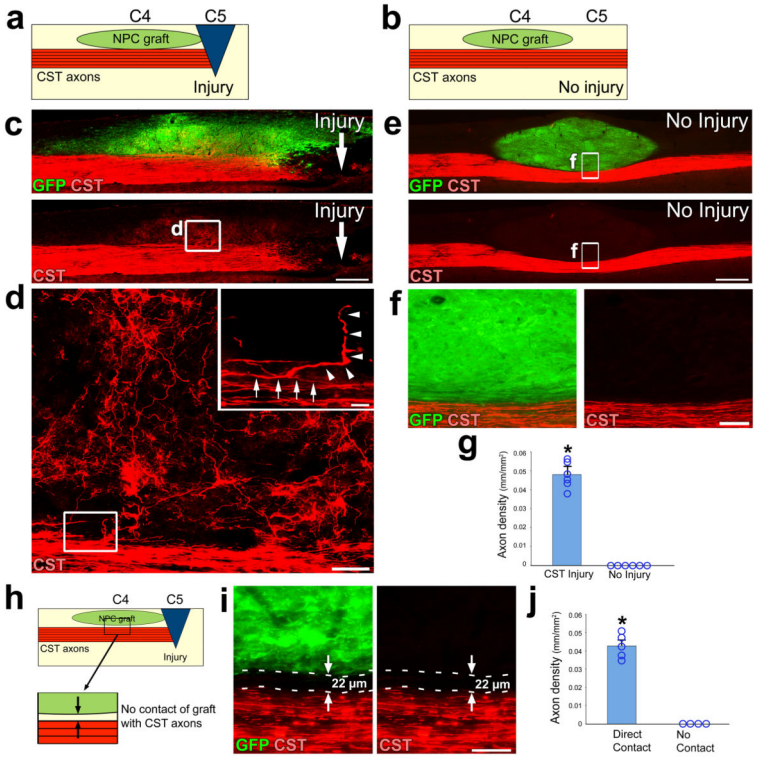

Figure 4. Corticospinal regeneration requires an injury signal and contact with neural grafts

(**a**–**b**) Experimental design to determine the requirement of an injury signal to enable CST axon regeneration. NPC grafts were placed into the spinal sensory columns at C4 immediately dorsal to the CST. In injured animals (**a**), a spinal cord lesion was placed at C5 transecting the dorsal corticospinal projection. “No injury” animals did not receive a lesion (**b**). (**c**–**f**) Low and high magnification views of BDA-labeled CST axons (red) with GFP-expressing NPC graft (green) in the presence of (**c**, **d**) or absence of (**e**, **f**) CST injury. Rostral is left, caudal is right. Scale bars: **c**, **e**, 500 µm; **d**, 50 µm; **f**, 100 µm. (**d**) High magnification views of boxed area in **c** depicts a corticospinal axon in the main tract (arrows, inset) that gives off a branch (arrowheads, inset) which penetrates the graft (inset; scale bar, 10µm). (**f**) High magnification of boxed area in **e**. (**g**) Quantification of CST axon regeneration into grafts with or without C5 injury. *P<0.01, Wilcoxon test. (**h**) Experimental design to determine the requirement of physical contact between the NPC graft and injured CST axons. NPCs are grafted to C4 and a spinal cord injury is placed at C5 (as in **a**), but in some cases with a 22–50µm gap interposed between the graft and the CST. (**i**) High magnification views of a 22 µm gap between NPC graft and injured CST axons. Scale bar, 50 µm. (**j**) Quantification of CST axons in grafts with or without direct contact of grafts with CST. *P<0.01, Wilcoxon test. Error bars represent mean ± s.e.m. and circles indicate data from individual rats throughout.

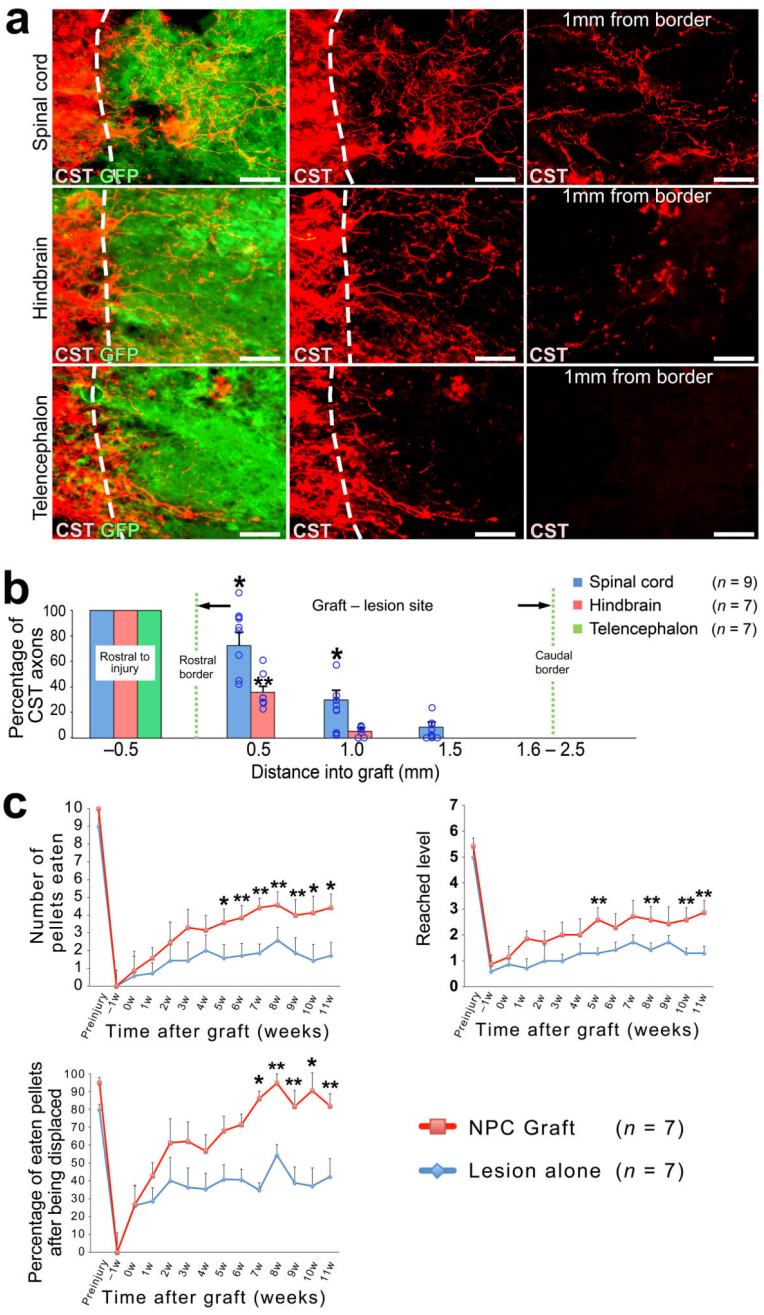

Figure 5. Corticospinal regeneration requires caudalized, homotypic grafts and enables functional improvement

(**a**, **b**) To determine whether homology of graft tissue to the spinal cord is required for corticospinal regeneration, we placed CST lesions at C4 and grafted NPCs derived from either E14 rat spinal cord (upper panels), hindbrain (middle panels) or telencephalon (lower panels). Sagittal sections were double labeled for CST axons (red) and NPC graft (green). Dashed lines indicate rostral host/graft border. Scale bar, 50 μm. (**b**) Quantification of the proportion of CST axons in NPC grafts, normalized to the total number of CST axons 0.5mm rostral to the lesion site in six rats. ANOVA P<0.01; post hoc, *P<0.05 to hindbrain

and telencephalon, **P<0.05 to telencephlon. Kruskal-Wallis ANOVA with post hoc Steel-Dwass test. Circles indicate data from individual animals. (**c**) Behavioral outcomes on staircase test after C4 right quadrant lesions and NPC grafts. Number of pellets eaten (upper left); repeated measures ANOVA P<0.05 with post-hoc Fischer's on individual days indicated by asterisks; *P<0.01, **P<0.05. Maximum depth of staircase reached (upper right) and pellet grasping accuracy (lower right): repeated measures ANOVA P = 0.07 on both tasks; exploratory post-hoc Fischer's shown with *P<0.01, **P<0.05. Throughout, error bars represent mean ± s.e.m.

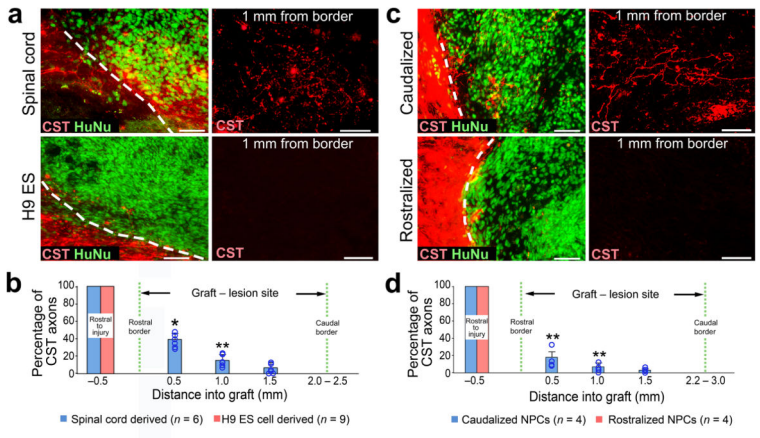

Figure 6. Homotypic human NPC grafts support corticospinal regeneration

(**a**) Sagittal views of human NPC grafts derived either from spinal cord (upper panels), or from the H9 ESC line driven toward a rostral midbrain fate (lower panels) placed at C4 CST injury in immunodeficient rats. Graft cells are labeled with human nuclear marker (HuNu, green) and CST axons are BDA labeled (red). (**b**) Quantification of proportion of CST axons in NPC grafts, normalized to total number of CST axons 0.5mm rostral to lesion site. $n = 6$ rats, spinal cord-derived grafts. $n = 9$ rats, H9 ESC-derived grafts. Wilcoxon test, *P<0.01, **P<0.05. (**c**) Sagittal views of human NPC grafts comprised of either caudalized (hindbrain, upper panels) or rostralized (forebrain, lower panels) NPCs derived from human induced pluripotent stem cells (iPSCs) placed in C4 CST lesion sites in immunodeficient rats. (**d**) Quantification of the proportion of CST axons in NPC grafts, normalized to the total number of CST axons 0.5mm rostral to the lesion site. $n = 4$ rats each for caudalized or rostralized iPSC-derived grafts. Wilcoxon test, **P<0.05. Throughout, rostral is left, dashed lines indicate rostral host/graft border. Scale bars, 50 μm for all images. Error bars represent mean ± s.e.m and circles indicate data from individual animals, throughout.